Materials Transactions, Vol. 46, No. 12 (2005) pp. 2975 to 2980

Abnormal Grain Growth of Off-Cube Grains in High Purity Aluminum Foils with Cube Texture*[1]

Naoki Takata[1,*2], Fuyuki Yoshida[2,*3], Ken-ichi Ikeda[2], Hideharu Nakashima[2] and Hiroshi Abe[2]

[1]*Interdisciplinary Graduate School of Engineering Science, Kyushu University, Kasuga 816-8580, Japan*
[2]*Faculty of Engineering Sciences, Kyushu University, Kasuga 816-8580, Japan*

In present study, abnormally coarsened grains in high purity aluminum foils with cube texture ({100}⟨001⟩) after a final annealing was investigated using SEM/EBSP method. Most of abnormally coarsened grains had Goss ({110}⟨001⟩) or S ({123}⟨634⟩) orientations. The coarsened grains with Goss and S-orientations were surrounded by $\Sigma 5$ and $\Sigma 7$ coincidence boundaries, respectively. This result clarified that these coincidence boundaries would enhance the abnormal grain growth of Goss and S oriented grains. Grain boundary energy of sub-boundaries between cube-oriented grains provided the driving force for the abnormal grain growth. The distribution of Goss oriented grains in the partially annealed foils was characterized by SEM/EBSP method. This characterization revealed that many Goss-oriented grains were distributed in the transition band on the central layer of the sheets.

(Received June 15, 2005; Accepted September 20, 2005; Published December 15, 2005)

Keywords: *goss texture, cube texture, grain growth, grain boundary character, grain boundary migration, secondary recrystallization*

1. Introduction

It has been generally known that cube texture ({100}⟨001⟩) is a main component of recrystallized texture[1)] in pure aluminum and its alloys, which is closely related to forming or etching property. Several thermo-mechanical processes have been developed for the control of cube texture in commercially pure aluminum and its alloys. A thermo-mechanical process through a cold rolling, a partial annealing (the annealing temperature is 240–260°C), an additional rolling (the reduction in thickness is approximately 20%) and a final annealing has been developed for the formation of sharp cube texture in a high purity aluminum and an Al–Mn–Mg alloy,[2)] which are referred to as Pechiney process.[3)] This process is the production process for aluminum foils for electrolytic capacitors.

The mechanism of preferential growth of cube-oriented grains (cube grains) by the Pechiney process has been investigated using SEM/EBSP method.[4,5)] The previous investigations have clarified that the difference of accumulated strains between cube grains and off-cube grains induced by an additional rolling could provide the driving force for the preferential growth of cube grains during the final annealing. This mechanism is expected to have come from the property that cube grains have less accumulated strains than off-cube grains.[6)] Hence Controlling the formation of substructure accelerated the preferential growth of cube grains and inhibited growth of off-cube grains, leading to the production of higher volume fraction of cube texture more than 95%.[7)] However, in some cases, off-cube grains abnormally grow to over 10 cm in grain size in high purity aluminum sheets through the Pechiney process, and bring about decline of a volume fraction of cube texture. Most of recent studies[8–14)] are concerned to the preferential growth of cube grains, so that there are few studies on the character of residual off-cube grains in aluminum sheets with cube texture. Accordingly, establishing the mechanism of the formation and growth of off-cube grains in aluminum sheets with cube texture is important for not only the development of processes for control of cube texture but also understanding the fundamental mechanism of cube texture development in aluminum and its alloy.

In the present study, off-cube grains in high purity aluminum foils with cube texture were analyzed by SEM/EBSP method. From the results, the mechanism of abnormal growth of off-cube grains is discussed focusing an attention to mobility and driving force of grain boundary migration between cube grains and off-cube grains. A distribution of orientation in aluminum foils before the final annealing was characterized by SEM/EBSP method. Comparing the distribution of off-cube grains in the foils before and after the final annealing, we discuss the mechanism of the formation of off-cube grains during the thermo-mechanical process.

2. Experimental

2.1 Samples

Aluminum foils of 99.9% purity, which were trial products by SHOWADENKO K. K., were used for samples in the present study. The aluminum foils contained 17 ppm Fe, 23 ppm Si and 39 ppm Cu. Hot rolled plates, 10 mm in thickness, were cold rolled to about 230 μm, then were annealed at 240 or 250°C for 6 h in air. These sheets were denoted as partial annealed foils. The partial annealed foils were cold rolled to 184 μm in thickness. The foils were denoted as additionally rolled foils. The additionally rolled foils partially annealed at 240°C were annealed at 540°C for 24 h. These foils were denoted as finally annealed foils. Figure 1 shows the production process of samples.

2.2 Measurement of SEM/EBSP method

A partially annealed foil was cut into $5 \times 10\,\mathrm{mm}^2$ for the measurement by SEM/EBSP method. A surface of the foil

*[1]This Paper was Originally Published in Japanese in J. JILM. **54** (2004) 573–578.
*[2]Graduate Student, Kyushu University
*[3]Present address: Nakayama Steel Works, ltd., Osaka 511-8551, Japan

was electropolished to prepare sample for a observation of ND plane. A surface for a observation of TD plane was mechanically polished then electropolished. The electropolishing was performed at 2°C with DC Voltage of 20 V and a mixture of perchloric acid, ethylene glycol and ethyl alcohol of 1:2:7 in volume ratio. A finally annealed foil was etched using the aqua regia mixed by hydrochloric acid and nitric acid of 3:1 in volume ratio in order to recognize off-cube grains in the sheets with cube texture. The etched sheets were cut and electropolished for the measurement by SEM/EBSP method.

The measurement of orientation by SEM/EBSP method was carried out using SEM (JEOL JSM-5310), equipped with TSL OIM (Orientation Imaging Microscopy) system. The accel voltage was 25 kV and the scanning step were 1–5 μm.

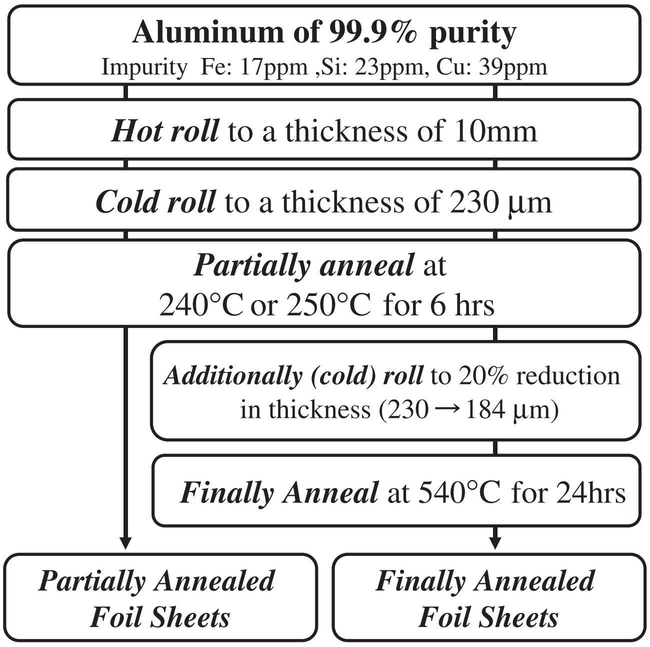

Fig. 1 Production process of samples.

The measurements of each sample were carried out more than three times. Using the measured data, a distribution of orientations and the grain boundary character were analyzed by TSL software (OIM Analysis).

3. Results and Discussion

3.1 Crystallographic characteristics of off-cube grains

Figure 2 shows an optical image of a final annealed foil etched by the aqua regia. This figure shows that off-cube grains abnormally grow, leading to decline of cube texture in volume fraction. In the figure, dark indicates to regions with ⟨100⟩ // ND. On the other hands, bright indicates to regions without ⟨100⟩ // ND, which prove off-cube grains. It is recognized that the foil had exceedingly large regions with off-cube orientations. And there are many off-cube grains whose size is 100–500 μm in cube texture of the foil, as shown by a circle in Fig. 2.

Figure 3 shows an OIM image and the pole figures of off-cube grains in the final annealed foils. In Fig. 3(a), gray colored area indicates cube grains whose misorientation angle from ideal cube orientation ({100}⟨001⟩) is less than 15

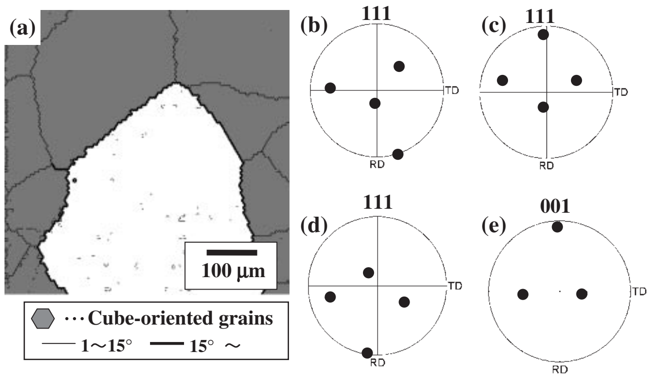

Fig. 3 OIM Images and pole figures of off-cube oriented grains (grain size $d = 100$–500 mm) in the finally annealed foils (partially annealed at 240°C).

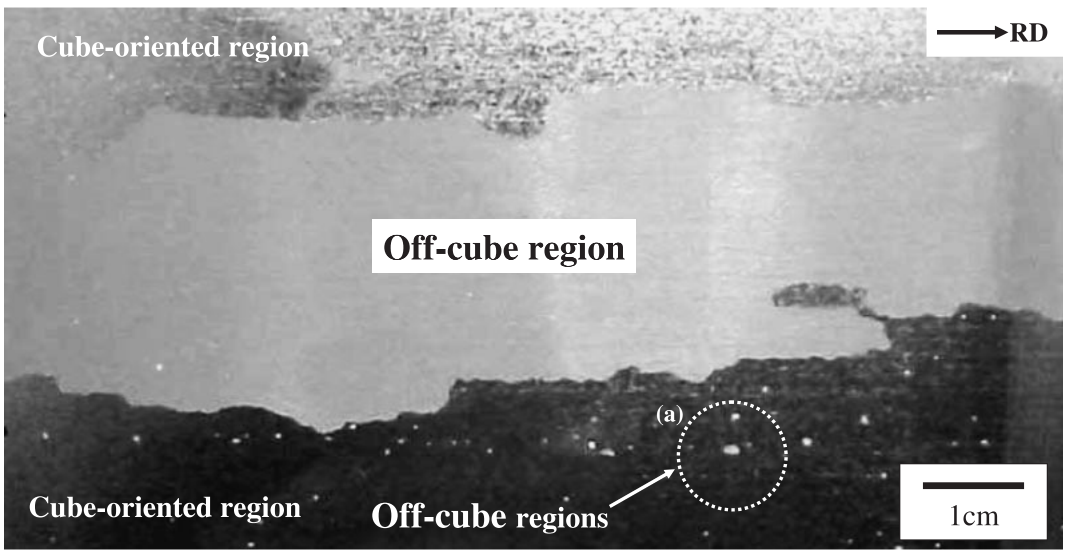

Fig. 2 A finally annealed foil sheet (partially annealed at 240°C) which has large regions with off-cube orientation.

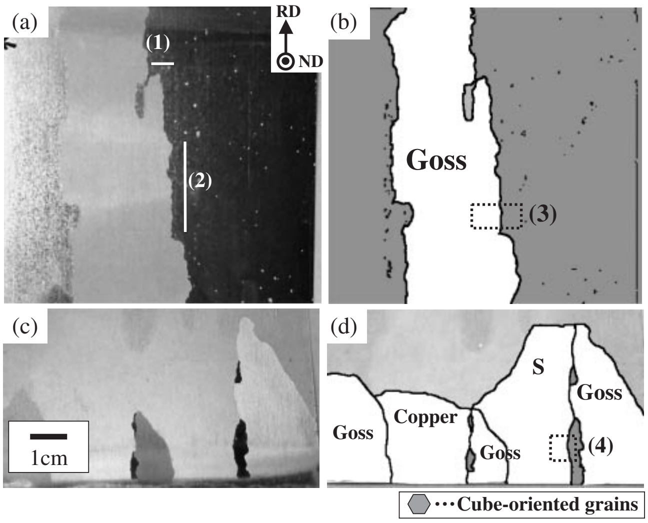

Fig. 4 Optical micrographs and orientation distribution maps in the finally annealed foils.

degrees, which is defined as cube grains in the present study. The area with cube orientation is subdivided by low-angle boundaries to 260 μm in mean diameter. Off-cube grains are surrounded with high angle boundaries. Many off-cube grains have Copper orientation ({112}⟨111⟩) or S orientation ({123}⟨634⟩) corresponding to β-fiber components,[15] which is a typical rolling texture in aluminum, are shown in Figs. 3(b) and (c). Some off-cube grains did not belong to β-fiber components, as shown in Fig. 3(d), but are comparatively close to Copper orientation or S orientation. Figure 3(e) shows that a small number of off-cube grains are Goss orientation ({110}⟨001⟩). These results indicate that most off-cube grains 100–500 μm in size, which remain in finally annealed foils, are typical rolling texture components.

Figure 4 shows optical micrographs and orientation distribution maps of the finally annealed foils, in which observed off-cube grains coarsen to over 10 mm. Each orientation of off-cube grains is denoted in Figs. 4(b) and (d). These figures shows that many coarsened off-cube grains had Goss and S orientation in the finally annealed foils. This result is apparently different to that of off-cube grains with size of 100–500 μm.

Figure 5 shows the frequency of the number of off-cube grains in the final annealed foils. The off-cube grains are classified in accordance with grain size d. In the present study, a tolerance of misorientation angle from the ideal orientations is defined as 15 degrees for the determination of Brass, Copper and Goss orientation, and 5 degrees for S orientation, respectively. Figure 5 indicates that 40% of off-cube grains with size of 100–500 μm belong to β-fiber components such as Copper and S orientation. While 50% of that can be classified to other orientations. After precise analysis, these grains are close to Copper and S orientation, as shown in Fig. 3(d). On the contrary, more than 70% of off-cube grains with size of over 10 mm had Goss or S orientation. These results provide an clear evidence that the abnormal grain growth preferentially occurs in Goss-oriented grains and S-oriented grains during the final annealing.

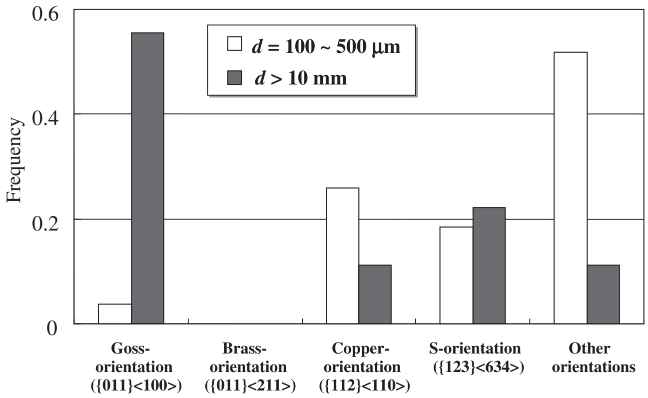

Fig. 5 Frequency of crystal orientation of off-cube oriented grains in the finally annealed foils (d: grain size).

3.2 Grain boundary character and driving force for abnormal grain growth

It has been generally accepted that a rate-controlling process of grain growth is a grain boundary migration. The velocity of grain boundary migration, v, can be given by the following equation.[16)]

$$v = M \cdot P \tag{1}$$

Here M and P represent mobility and driving force for the grain boundary migration, respectively. The mobility is affected by the impurity[17)] and grain boundary character.[18,19)] It is expected that the stored energy caused by accumulated dislocations, grain boundary energy or surface energy can provide the driving force. Accordingly, the driving force for the abnormal grain growth and grain boundary character are discussed for investigation of the mechanism of abnormal growth of Goss and S-oriented grains, as are described in the follow section.

Figures 6(a) and (b) show a distribution map of cube grains and a 001 pole figure of the region (3) in Fig. 4(b), and Figs. 6(c) and (d) show a distribution map of cube grains and

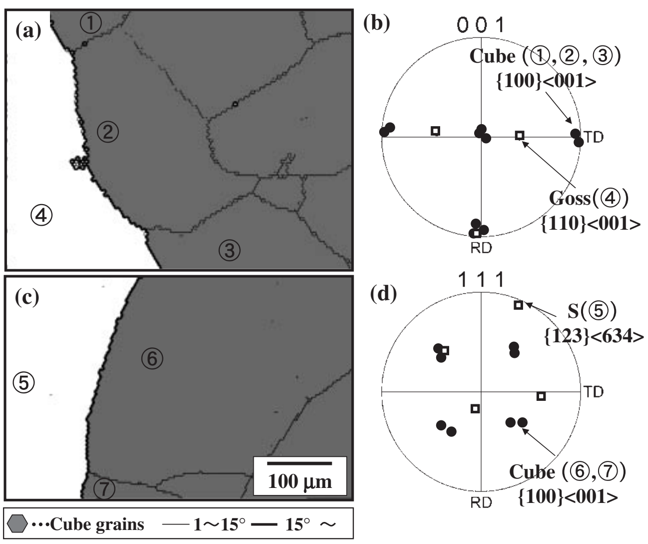

Fig. 6 OIM Images for (a) (c) the distribution of cube-oriented grains and (b) (d) pole figures in the finally annealed foils (partially annealed at 240°C).

a 111 pole figure of region (4) in Fig. 4(d), respectively. In Figs. 6(a) and (c), thin lines correspond to misorientation of 1–15 degrees and thick lines to over 15 degrees, respectively. The cube grains are composed of sub-grains with size of 100–500 µm and low angle boundaries with the average misorientation of 8 degrees, as shown in Figs. 4(b) and (d). The large region with Goss or S orientation consisted of a single grain. Preliminary experiments revealed that the coarsened grains were not observed in foils finally annealed for as short as 60 s. Thus these experiments support the understanding that the abnormal grain growth dose not occur at stage of primary recrystallization. It is therefore concluded that a Goss or S-oriented grain abnormally grew consuming the cube grains during the final annealing.

Figures 6(b) and (d) show that pole figures of coarsened off-cube grains and neighboring cube grains in the finally annealed foils. The figures indicate that the orientation relationship between cube grains and off-cube grains. A coarsened Goss-oriented grain is surrounded by grain boundaries with a common axis of ⟨100⟩ and the misorientation angle of about 45 degrees, as shown in Fig. 6(b). The orientation relationship is close to $\Sigma 5$ coincide relationship. Most of these grain boundaries fulfill the Brandon criterion[20] that defined a tolerance of coincidence boundaries. And the grain boundaries of a coarsened S-oriented grain have a misorientation of 40 degrees with a ⟨111⟩ axis, which corresponded to $\Sigma 7$ coincidence boundary, as shown in Fig. 6(d). It is found that grain boundaries of coarsened off-cube grains had the special orientation relationship with low Σ values. Many experimental results have shown that there was a large dependence of mobility on misorientation.[17,21,23] There were considerable evidences[22,23] that the minimum activation energy which occurs close to misorientations of 37 and 38 degrees on ⟨100⟩ and ⟨111⟩ axis respectively, was consistent with the maximum mobility in pure f.c.c. metals. It is therefore concluded that the abnormal grain growth during the final annealing could preferentially occur in only Goss and S-oriented grains with grain boundary of the special orientation relationship with cube grains.

Particularly, Fig. 4(a) indicates that Goss-oriented grains have been preferentially growing to RD rather than TD. The boundaries can be therefore classified to twist boundaries (1) and tilt boundaries (2) in Fig. 4(a). Figure 7 shows schematic illustrations of a twist boundary (a) and a tilt boundary (b). From Fig. 7, the grain boundary planes of the tilt boundary correspond to $(010)_{Cube}$ // $(110)_{Goss}$ in cube grains and a Goss-oriented grain. On the other hand, that of the twist boundary correspond to $(001)_{Cube}$ // $(001)_{Goss}$ in cube grains and a Goss-oriented grain. Fig. 4(a) clearly shows that the twist boundaries preferentially migrated rather than the tilt boundaries in $\Sigma 5$ coincidence boundaries of Goss-oriented grains. Since grain boundary dislocations play a significant role of the grain boundary migration,[24,25] this preferential migration can be explained by a element of the grain boundary dislocations. The motion of screw dislocations in twist boundaries is not necessarily for the climb by diffusion and associated steps in grain boundaries. And it has been generally accepted that the hydrostatic pressure which comes form edge dislocations would bring out a interaction between the edge dislocations and segregated atoms.[26] Hence, the impurity segregated in grain boundaries suppresses the motion of edge dislocations. These facts suggest that screw dislocations could move more easily than edge dislocations. Thus the anisotropy of abnormal grain growth shows that the mobility of each dislocation affects the velocity of grain boundary migration. It is therefore concluded that the behavior of the abnormal grain growth was affected not only by the Σ value but also by the grain boundary plane.

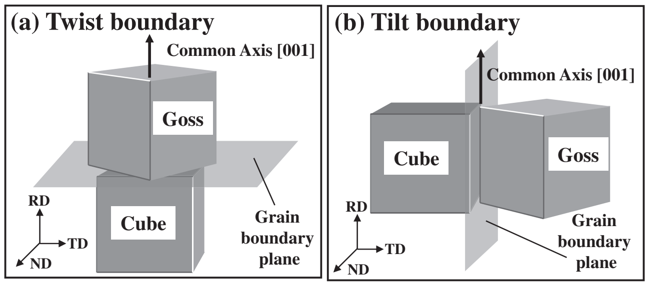

Fig. 7 Schematic illustrations of (a) a twist boundary and (b) a tilt boundary between an ideal cube orientation ({100}⟨001⟩) and an ideal Goss orientation ({110}⟨001⟩).

Table 1 surface energy (J/m^2) of aluminum reported.

	{001}	{011}	{111}
J. Schochlin *et al.*[27]	1.081	1.090	0.939
B. Mutasa and D. Farkas[28]	0.935	0.980	—

It is predicted that there are not the accumulated strains in cube or off-cube grains which play a role of the driving force for the primary recrystallization, because the final annealing for long time is necessary for the occurrence of abnormal grain growth. The prediction is supported by the result that there were low misorientation in recrystallized grains in final annealed foils, as was shown in Figs. 3 and 6. These prediction can lead to a prospect that the diving force at final annealing is a energy of sub-boundaries between cube grains or a difference of surface energies. Table 1 shows the surface energy of each plane in pure aluminum reported.[27,28] These previous studies revealed that a {011} surface plane has slightly higher energy than a {001} surface plane, which indicates that the surface energy cannot play a role in the driving force for abnormal grain growth. Whereas, focusing an attention on triple junctions composed of coincidence boundaries and sub-boundaries, coincidence boundaries are curved and the sub-boundaries between cube grains are shrinking, as shown in Figs. 6(a) and (c). These morphologies can explain that the energy of sub-boundaries between cube grains promotes the migration of coincidence boundaries surrounding Goss and S-oriented grains. Consequently, it is assumed that a energy of sub-boundaries between cube grains provided for the driving force of the abnormal grain growth.

It has been generally accepted that the stored energy due to accumulated strains is about 10^3 times as large as grain boundary energy.[29] Thus we propose an understanding that the grain growth driven by large force such as the stored energy was little affected by the mobility of grain boundary, while that by small force due to grain boundary energy

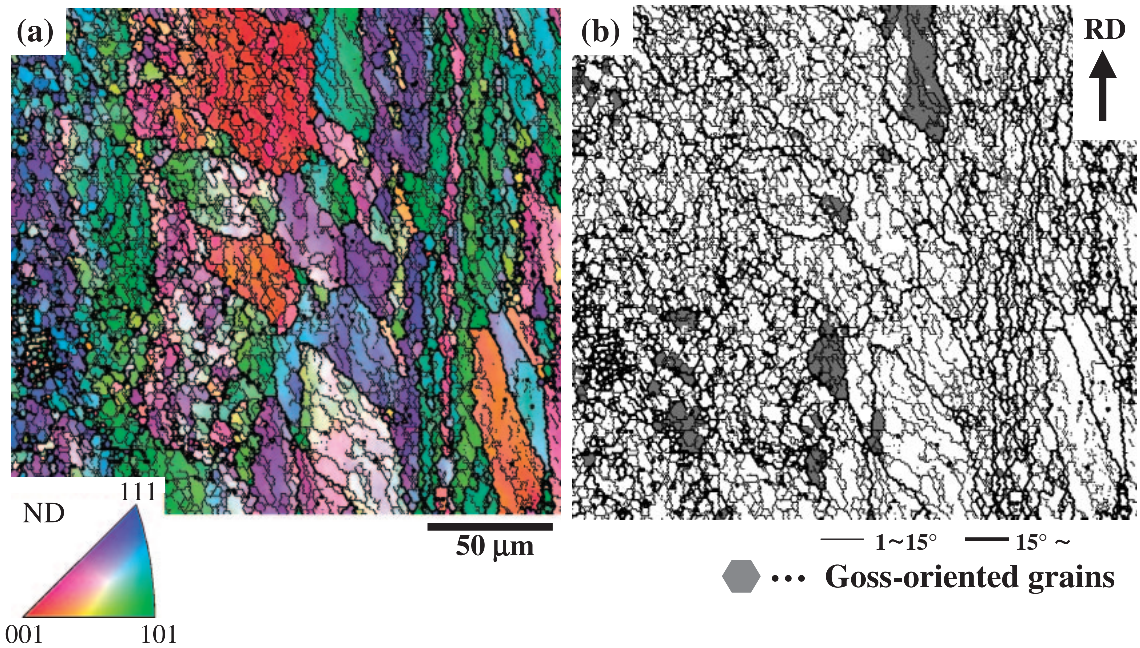

Fig. 8 OIM image for (a) crystal orientations and (b) distribution map of Goss-oriented grains in a transverse section of foils partially annealed at 250°C.

strongly depended on the mobility. This understanding also agrees well with the experimental result that grain boundary character had little influence on the behavior of grain growth driven with the stored energy.[4,5,14]

From above-mentioned results, we draw a conclusion that the abnormal grain growth during the final annealing is caused by the selective growth, among various off-cube grains, of Goss and S-oriented grains, which have coincidence boundaries with high mobility, driven by the energy of sub-boundaries between cube grains which predominantly existed in stage of final annealing.

3.3 Relationship between the formation of off-cube grains and deformation microstructure

In the previous section, it has been described that most of abnormally coarsened grains had Goss and S orientations. S-orientation is one component of deformation texture caused by a heavily cold rolling (β-fiber). Hence S-oriented grains can be thought to form within the deformed or recovery microstructure and then remain in cube texture during the final annealing. But Goss-oriented grain is not a main component of rolled texture and has been scarcely observed in cold rolled foils.[4,14] Therefore it can be expected that the formation mechanism of Goss-oriented grains is different from that of S-oriented grains. For the investigation of formation mechanism of Goss-oriented grains during the thermo-mechanical process, microstructure in the partial annealed foils was characterized by SEM/EBSP method.

Figure 8 shows OIM images for the orientation and Goss orientations on the transverse section in the partial annealed foils. Figure 8(a) is colored according to the unit triangle, which corresponds to the inverse pole figure of ND. Goss-oriented grains indicated the gray regions in Fig. 8(b). It is recognized that both morphology and size of microstructure changed depending on a thickness of the partially annealed foils. It could be expected that relatively inhomogeneous microstructure, which was formed by the cold rolling, have recovered or partially coarsened during the partial annealing. There were some relatively coarsened banded structures in the center layer of the partial annealed foils. This banded structure inclined approximately ±40 degrees to the rolling plane. Many Goss-oriented regions were observed in this banded structure. This banded structure is assumed to be the transition band in the deformation microstructure. The transition band is characterized by the orientation gradient bridging some texture components,[30] since a microscopic inhomogeneity occurs in the transition band instead of evolution of deformation band parallel to RD. Thus the distribution of accumulated strains was inhomogeneous in the transition band. That lead to the prediction that fine grains in the transition band grew faster than those in other regions. These results suggest that Goss-oriented grains locally generate by inhomogeneous deformation during the cold rolling. Hjelen *et al.*[30] also have observed the preferential growth of Goss-oriented grains in the transition band in aluminum sheets of 99.99% purity rolled to the reduction of 90–95%. This previous work supports the results in this study. It is accordingly proposed that Goss-oriented regions locally generated in the transition band in contrast to S-oriented grains. Accordingly, these results suggested that the formation of Goss-oriented grains could be suppressed by the development of the suitable cold rolling condition for the minimization of inhomogeneous deformation microstructure.

4. Conclusion

In order to clarify the mechanism of abnormal grain growth of off-cube grains in aluminum foils with cube texture by performing the Pechiney process, the distribution of orientation and grain boundary character was analyzed by SEM/EBSP method. The results are summarized as follows.

(1) Most of coarsened grains in the final annealed foils had Goss and S orientations and were surrounded by $\Sigma5$ and $\Sigma7$ coincidence boundaries, respectively. It was clarified that the migration of the coincidence boundaries with low Σ value enhanced the abnormal grain growth during the final annealing. The driving force for the abnormal grain growth is expected to be the energy of sub-boundaries between cube grains.

(2) Goss-oriented grains which were expected to grow abnormally, were distributed in the transition band in the central layer of the partial annealed foils.

Acknowledgements

The authors would like to thank Mr. K. Yoshida, Mr. M. Sakaguchi and Mr. T. Yamanoi for their help of experimental works and fruitful advice.

REFERENCES

1) F. J. Humphrey and M. Hatherly: *Recrystallization and Related Annealing Phenomena*, (Pergamon, 1995) pp. 327–362.
2) T. Takahashi, T. Murakami and N. C. Danh: J. JILM **28** (1978) 35–40.
3) F. Seki and T. Kamijo: J. JILM **48** (1998) 507–510.
4) K. Ikeda, K. Tumagari, F. Yoshida, H. Nakashima and H. Abe: J.JILM **51** (2001) 119–124.
5) F. Yoshida, K. Ikeda, N. Takata and H. Nakashima: *Proceedings of the 25th Riso International Symposium on Material Science* (2004) 571–576.
6) M. Tagami, K. Kashihara, T. Okada and F. Inoko: Mater. Trans. **42** (2001) 2013–2020.
7) N. Takata, K. Ikeda, F. Yoshida, H. Nakashima and H. Abe: J. JILM **53** (2003) 218–223.
8) Q. Cui, H. Saitoh and K. Ohori: J. JILM **49** (1999) 583–588.
9) T. Kamijo, F. Seki, H. Tamai and K. Ito: J. JILM **49** (1999) 589–594.
10) O. Engler and M. Y. Huh: Mater. Sci. Eng. A **271** (1999) 371–381.
11) K. Kajihara, K. Tokuda, Y. Sugizaki and Y. Seki: J. JILM **51** (2001) 182–187.
12) S. Endo and H. Inagaki: J. JILM **52** (2002) 167–173.
13) M. Kobayashi, Y. Takayama and H. Kato: Mater. Trans. **45** (2004) 3247–3255.
14) N. Takata, K. Ikeda, F. Yoshida, H. Nakashima and H. Abe: Mater. Trans. **45** (2004) 1687–1692.
15) J. Hirsch and K. Lucke: Acta Metal. **36** (1988) 2863–2882.
16) R. C. Sun and C. L. Bauer: Acta Metall. **18** (1970) 635–638.
17) K. T. Aust and J. W. Rutter: Trans. Metall. AIME **215** (1959) 119–127.
18) H. Nakashima, T. Ueda, S. Tsurekawa, K. Ichikawa and H. Yoshinaga: Testu-to-Hagane **82** (1996) 238–243.
19) F. Yoshida, M. Uehara, K. Ikeda, H. Nakashima and H. Abe: Mater. Sci. Forum **467–470** (2004) 835–840.
20) D. G. Brandon: Acta Metall. **14** (1966) 1479–1482.
21) J. W. Rutter and K. T. Aust: Acta Metall. **13** (1965) 181–186.
22) D. W. Demianczuk and K. T. Aust: Acta Metall. **23** (1975) 1149–1162.
23) D. A. Molodov, J. Awiderski, G. Gottstein, W. Lojkowski and L. S. Shvimderman: Acta Matell. Mater. **42** (1994) 3397–3407.
24) R. W. Balluffi and J. W. Chen: Acta Metall. **29** (1980) 493–500.
25) C. M. F. Rae and D. A. Smith: Philos. Mag. A **41** (1980) 477–492.
26) P. Haasen: *Dislocations in Solids* (ed. by F.R.N. Nabarro North-Holland Publishing Company, 1979) Vol. 4, pp. 159.
27) J. Schochlin, K. P. Bohnen and K. M. Ho: Sur. Sci. **324** (1995) 113–118.
28) B. Mutasa and D. Farkas: Sur. Sci. **415** (1998) 312–319.
29) E. Furubayashi: *Saikessyou to Zairyousosiki* (in Japanese, Uchida Roukakuho, 2000), pp. 8.
30) J. Hjelen, R. Orsund and E. Nes: Acta Metall. **39** (1991) 1377–1404.